Lithographic Patterning and Etching of Diamond Metasurfaces

E241 Class Report – Spring 2022

Team: Hamish Carr & Matti Thurston

J. DIONNE LAB | STANFORD UNIVERSITY | MENTORS: VIJAY NARASIMHAN, J PROVINE, LAVENDRA YADAV MANDYAM

Table of Contents

Introduction

In recent years, the field of flat optics has seen considerable interest within the optical engineering community due to its potential to revolutionize technologies across a wide variety of industries and research fields. The reduction of the size of optical components has the potential to not only reduce cost and weight for current technologies but also enable major innovations in frontier fields such as AR/VR, quantum information science, LiDAR, and next generation telecommunications. In order to reduce component size, one area in which innovations have been proposed is through the use of metasurfaces.

Metasurfaces are nanoscale arrays of dielectric antennas that, through geometry-dependent functionalization, can alter the phase, amplitude, and/or polarization of incident light. By tailoring the material and geometry of a given metasurface to a specific wavelength of light, the resultant nanoarray can act as a beamsteerer, beamsplitter, or lens at much smaller length scales than traditional optics. Furthermore, due to local field enhancements observed in close proximity to the antennas, metasurfaces can serve as a means of enhancing optically addressable phenomena in coupled systems. This in turn has the potential to enable technologies dependent on everything from optically addressable qubits to chiral biomolecule sensors[1].

In order to enhance local field strength to a degree useful for certain technologies, metasurfaces must be patterned in a reliable and repeatable way to unlock high quality (high-Q) resonances. These resonances occur only when repeated geometric perturbations are introduced into the design of the antenna array. However, enhancement of the resonant characteristic is inversely proportional to the size of the introduced perturbation, meaning a highly reliable and nanometer resolution process is required to realize valuable resonances in the UV, visible, and near IR spectra[2].

The use of Silicon for metasurface design and patterning is well documented, and high Q beamsteerers and lenses have been demonstrated experimentally[3]. However, due to its optical properties, silicon cannot be leveraged in the UV and visible spectrum, meaning that an alternate material is required for innovations to be realized in that space. To that end, diamond has the potential to fill the gap; with its optical properties, high Q metasurfaces using diamond can potentially unlock technologies in the UV and visible range. Indeed, diamond metasurfaces have been demonstrated in the literature[4]; however, as of this publication, no high Q diamond metasurface has been fabricated, and little documentation exists on reliable processes to fabricate diamond metasurfaces at all.

In this report, we describe a process for the fabrication of high-quality factor metasurfaces on a diamond thin film platform. Following deposition of a metal hard mask and spin coating of a negative tone resist, electron beam lithography is utilized as a means of writing nanoscale features onto the material stack. By then using a series of etch steps, the mask is transferred into the diamond reliably and repeatably. Furthermore, we discuss our final material workflow in the context of lessons learned,

including an analysis of steps that were removed from our process. Finally, we discuss the implications of the final technology, and we provide an overview of the project as a lessons learned for future similar projects.

Benefit to the SNF / SNSF Community

As diamond becomes a material of increasing technological importance in a wide range of disciplines, the need for a method to reliably process diamonds becomes increasingly apparent. Due to its material properties, such as high thermal conductivity, high hardness, high refractive index and low loss in the visible and UV range, as well as its ability to host quantum defects, diamond has potential for applications in areas such as power electronics, photonics, and quantum information sciences, among others. However, to this day, diamond remains a challenging material to process as it is the hardest of all materials, and it is extremely chemically inert.

Throughout this class, we developed a process flow to reliably pattern diamond films or substrates using standard clean room fabrication techniques, such as electron beam lithography and reactive ion etching, leveraging tools at the Stanford Nanofabrication Facility (SNF) and the Stanford Nano Shared Facilities (SNSF) nanopatterning cleanroom.

We believe that the process that was developed will be beneficial to the SNF and SNSF community, as the documentation that we provide will be insightful and instructive to lab members that wish to fabricate diamond devices for their research. We hope that by providing a well-documented standard operating procedure to pattern diamond structures, research on various disciplines will be advanced and accelerated at Stanford.

Graphical Abstract - The Final Material Approach

In developing the process herein described, multiple inputs were taken into consideration. Of note, three primary sources were leveraged for developing the full-stack process, including: 1) Literature review (see references), in which diamond etching had been prior demonstrated; 2) Internal Lab review, in which expertise from the J. Dionne lab provided input on HSQ and e-beam writing; and, 3) Mentor input from the collaborative E241 team. It is important to note, as a consequence, that the multivariate nature of this process means optimizations do remain possible, and that choices of even things like the e-beam resist are partially due to in-house expertise over practice limitations.

While additional conversation is left to the Lesson's Learned section of this report, it is important to note further at this time that the final process leveraged in our diamond metasurface fabrication (Fig. 1) did not match our original proposal (Fig. 10). In the

process of tuning each fabrication step, certain pitfalls and gains were observed in switching to the final process presented here.

The resultant fabrication process flow is demonstrated below in Figure 1.

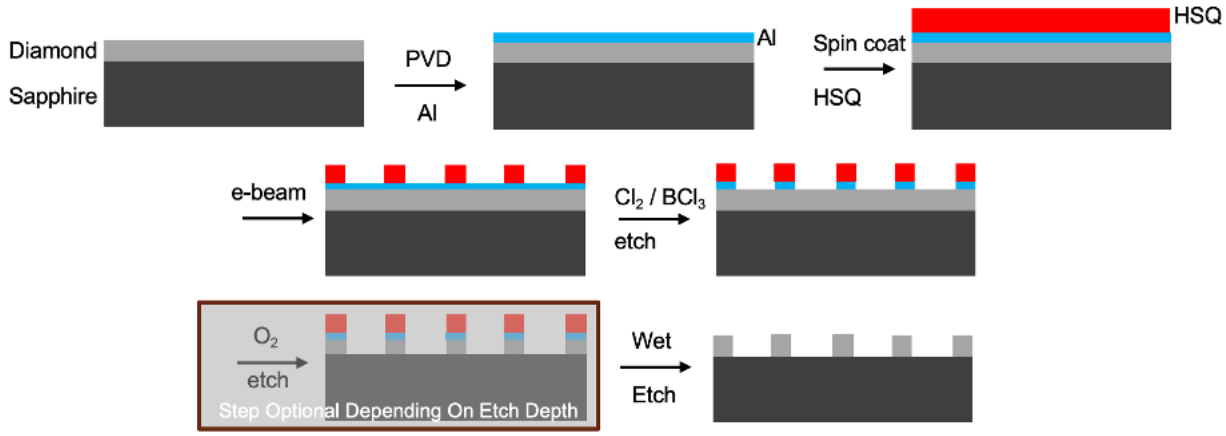

Figure 1: Graphical abstract of the diamond etch process developed within this report.

While detailed discussion is left to the rest of the report, a quick overview of the process is as follows:

1. Diamond films on substrate are selected; for optical devices usable in quantum and biophotonic applications, particular emphasis is put on the optical characteristics of the film (low loss, high refractive index) as well as the transmission characteristics of the substrate, in this case sapphire.

2. Aluminum (200 nm) is deposited through PVD on the surface of the diamond to serve as an eventual hard mask during the etch; alternative metals, such as Chromium, were also explored and could be usable with additional tuning. SNSF application of this process is performed through the KJL Sputter Deposition tool.

3. Hydrogen silsesquioxane (HSQ) is spin coated at 2000 RPM onto the Aluminum hard mask using the spinner benches in SNSF; HSQ is an electron beam negative tone resist that allows for the writing of high-resolution features.

4. E-beam lithography on the Raith Voyager is used to write the relevant metasurface pattern into the HSQ, resulting in its hardening into a silicon-rich oxide that itself serves as a mask. Remaining HSQ (non-developed) is removed through a salt bath.

5. A Chlorine / Boron Trichloride plasma etch is then performed in the PT-MTL Ox Etch system in SNF to etch away the Aluminum mask. These etches further

demonstrated the ability to etch away diamond directly, making the subsequent oxide etch optional depending on the nature of the etch being performed.

6. OPTIONAL: Depending on the exact material parameters under consideration, an additional etch using oxygen plasma in the Oxford RIE system in SNF can be used to etch away any remaining diamond and refine features.

7. A wet etch of BOE is used to remove any remaining materials, leaving behind only the diamond metasurface on substrate.

Additional modifications to the process are underway as of the writing of this report, and optimizations remain. Diamond etching of metasurfaces, however, is achievable with the process described herein.

Step I: Sample Input and Selecting the Right Diamond

As with any device fabrication, the process truly begins with the selection of the right input materials. For the implementation of high-quality diamond metasurfaces for such optical applications as those in quantum computing and biophotonics, the diamond being used should ideally demonstrate high uniformity to limit variability, low optical loss in the spectrum of consideration to reduce extinction, and high refractive index to allow for wider beamsteering angles. Many of these characteristics are dependent on the polycrystallinity and synthesis quality of the diamond being used; an ideal diamond film would be markedly monocrystalline and devoid of defects to reduce scattering pathways and ensure sample uniformity. Furthermore, as for any metasurface, control of the thickness of the diamond layer is crucial to the function of the device as metasurface function and optimization is geometry dependent. Consequently, films of uniform thickness and uniform etch characteristic are vital for this application.

It is important to note that substrate selection is crucial and non-trivial as well. Depending on if the device in question will be used in transmission or in reflectance, the substrate's optical characteristics are similarly important to limit extinction. Furthermore, the local dielectric properties associated with the substrate do alter the local field properties of the metasurface, meaning that any metasurface must be designed with the substrate in mind.

For this application, the original target material was determined to be monocrystalline diamond ($n = 2.42$, dielectric constant = 5.70, low extinction down to 250 nm) on a sapphire substrate. Sapphire was the target substrate to allow for transmission and low loss in the UV and visible spectrum, thus enabling the diamond metasurface in question to operate in either transmission or reflectance.

While an ideal target was set, modern diamond film deposition techniques tend to limit the ability to access monocrystalline regimes. Of note, even state of the art techniques

tend to lead to the deposition of polycrystalline samples, with the degree of polycrystallinity often determined by the thickness of the deposition (the thicker the deposition, the more dominant certain grains can become). Furthermore, growth on substrates like sapphire are currently non-scaled and only done in research settings, meaning sample availability is limited.

Thus, for the purposes of this report and debugging the process, fabrication was performed on commercial 100 nm polycrystalline diamond samples on 1 μm silicon oxide on silicon. These samples, purchasable through John Crane diamond, have optical properties in line with expectation as can be seen in the ellipsometry data in Figure 2**.** While not necessarily ideal for final metasurface realization, this material stack was determined to be sufficient to debug fabrication so that future iterations could be performed using higher quality materials linked with partner labs at Stanford and beyond.

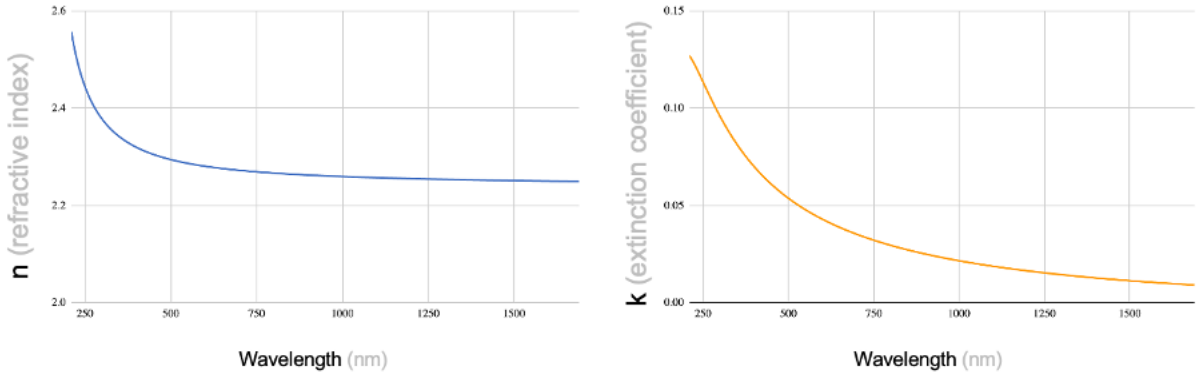

Figure 2: Elliposometry data of commercial diamond leveraged for the full stack etch process. On the left is refractive index as a function of incident wavelength; on the right is extinction coefficient. Ideal diamond thin films would show even lower extinction and higher refractive index.

Step II: Hard Mask Deposition

The rationale for using a hard mask is that diamond, being notoriously difficult to etch by chemical and physical methods, will require long, high power etches to fully transfer the desired pattern across the entire thickness of the diamond film. A metallic hard mask would provide more durability, compared to an e-beam resist mask. The initial process flow proposed the deposition of a thin 20 nm Cr hard mask and a thin SiO_2 film. The Cr mask would provide a hard stop for the O_2/Ar RIE etch to selectively etch diamond. The SiO_2 film was proposed to improve the adhesion of HSQ to the metal hard mask; however, this step was removed due to observed oxidation of the Cr film which made it more difficult to transfer the pattern into the metal mask.

After initial dry RIE etches, the Cr hard mask was found to be removed quickly by O_2 etches. Because of this, a thicker 200 nm Al hard mask was chosen due to reported use of this material as an etch mask for O_2/Ar etches. The 200 nm Al hard mask was also deposited using the KJL evaporator in SNSF, and thickness was confirmed with profilometry (Fig. 3).

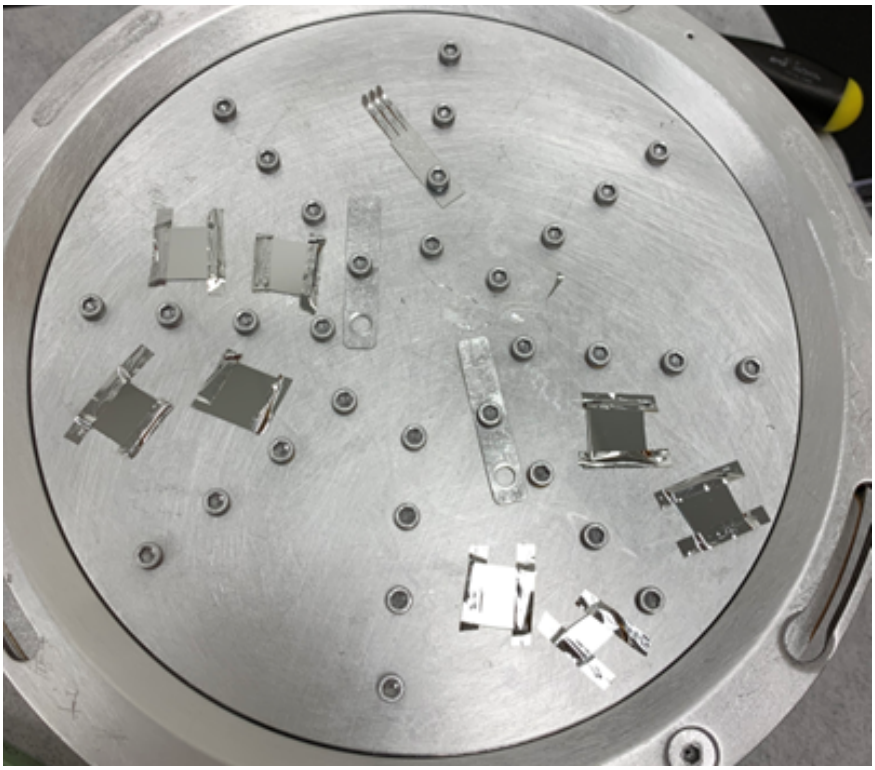

Figure 3: Image of blanket Aluminum films on diamond within the KJL evaporator

Step III: HSQ Spin Coat and Electron Beam Lithography

Hydrogen silsesquioxane (HSQ) was chosen as our electron beam resist. HSQ is a negative tone resist, meaning that the areas that are exposed to the electron beam become cured and act as an etch mask.

The sample preparation for e-beam lithography involves cleaning the samples in acetone and sonicating in isopropanol for 2 minutes. This is followed by a dehydration bake on a hotplate at 180° to ensure that water and solvent is evaporated from the sample. The next step is to spin coat HSQ onto the sample. This is done using the spin coater in the nanopatterning clean room. HSQ is spin coated on the samples at 2,000 RPM for 60 seconds. This results in a thickness of approximately 133.7 nm, according to the spin curve of 6% HSQ, shown below (Fig. 4). After spin coating, the solvent is evaporated by

a soft bake at 80° for 2 minutes. Then, e-spacer is spin coated on top of the HSQ at 2,000 RPM for 60 seconds, and, similarly, the solvent is evaporated by a 2 minute soft bake at 80°. Once this process is completed, the sample is ready to be patterned by e-beam lithography.

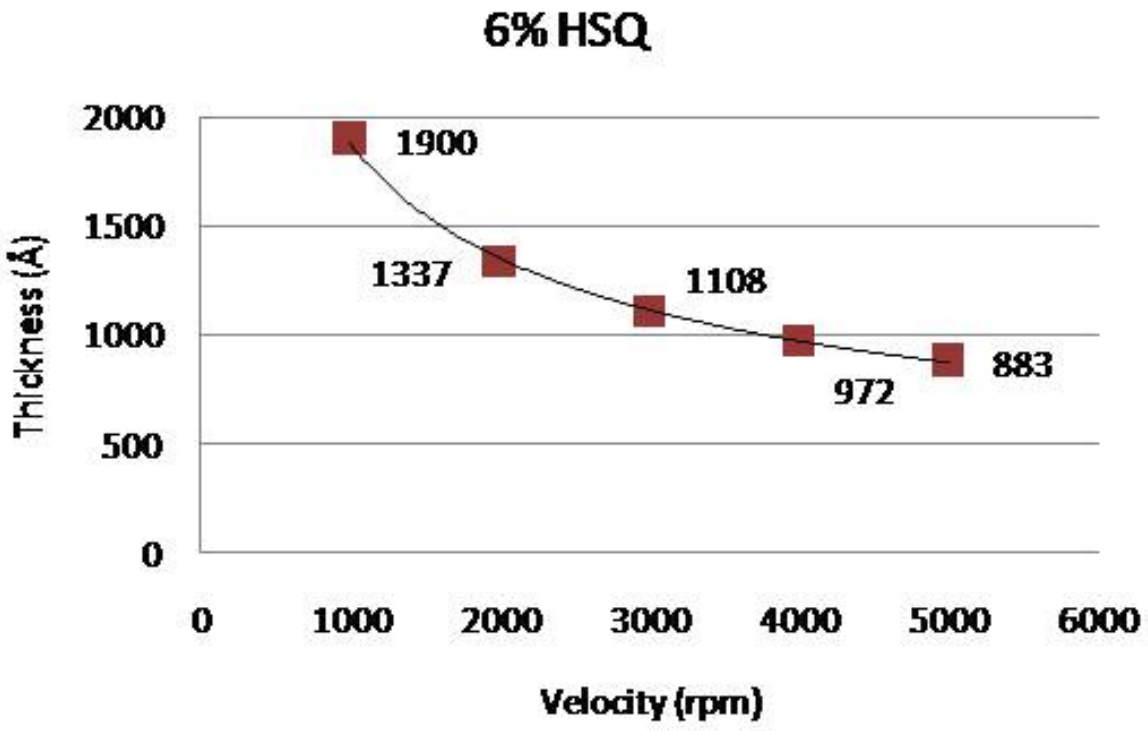

Figure 4: Image of HSQ spin curve thickness as a function of RPM. Courtesty of Georgia Tech.

The tool used for patterning was the Raith Voyager e beam lithography system in the SNSF nanopatterning clean room. The samples, which are 1 cm x 1 cm chips, are loaded on the Multi-Sample Holder, and a scratch is made on the corner of each chip for focusing and calibration of the electron beam. A 50 kV, 9 nA electron beam was used to pattern these samples, with a step size of 4.5 nm. The pattern that was designed consisted of nanobars of varying widths, ranging from 25 to 500 nm. In order to find the optimal dose for this pattern, a coarse dose sweep was performed, ranging from 2,000 - 7,000 μC/cm^2, in increments of 1,000. For this initial dose sweep, the best resolution was observed for doses ranging from 4,000 - 6,000 μC/cm^2. A subsequent finer dose sweep from 3,500 - 5,500 μC/cm^2, in increments of 200, revealed that the best resolution was obtained at a dose of 5,000 μC/cm^2.

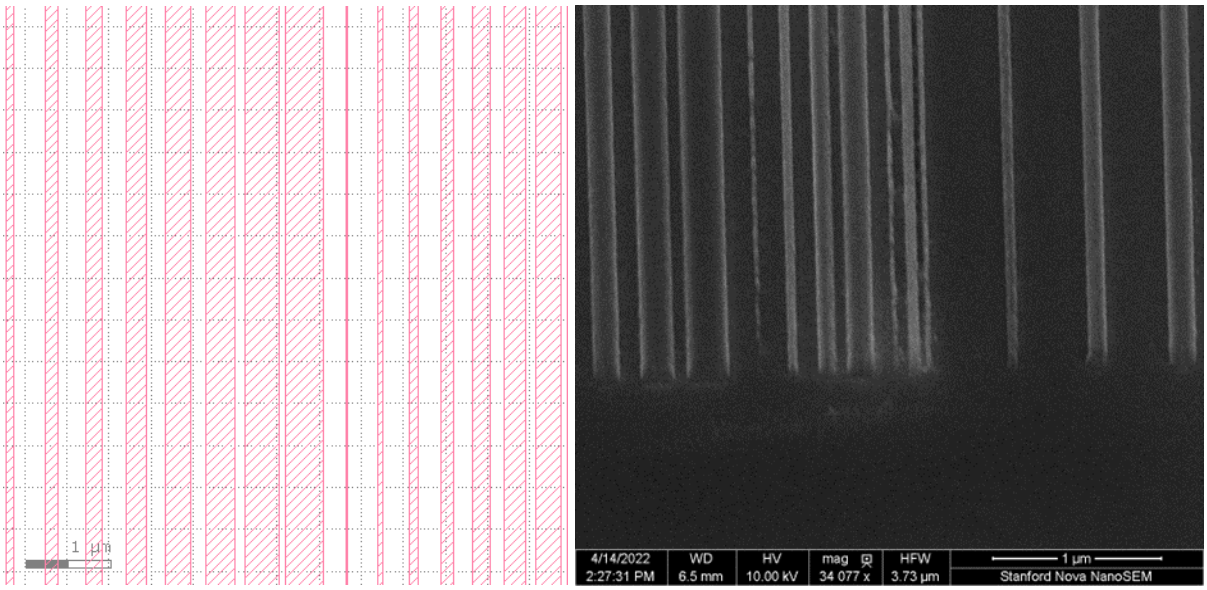

Figure 5: Implementation and result of the e-beam write. Left: Image of layout files of the pattern implemented within trial e-beam writes. Right: Result of write using 3,000 µC/cm^2, underexposed beam

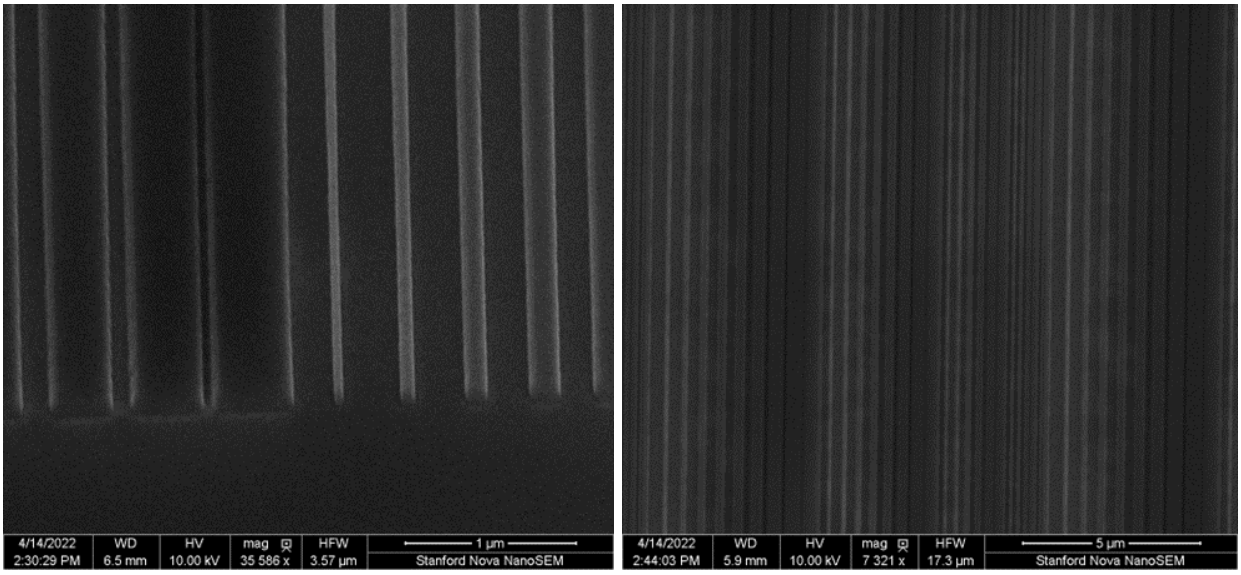

Figure 6: Two additional e-beam writes. Left: 5,000 µC/cm^2, Good resolution across sizes. Right: 7,000 µC/cm^2, Overexposed

After exposure, the chips were unloaded from the tool and developed in a solution of NaCl and NaOH to avoid the use of 25% TMAH. The composition of the developer solution is 95% DI water, 4% NaCl, and 1% NaOH, by weight. This solution was made outside the clean room in our own laboratory. The developing procedure begins by submerging the chip in a beaker of DI water for 30 seconds. This removes the e-spacer. After this, the chip is transferred to a beaker containing the developer solution for 2

minutes under mild agitation. This is followed by transferring the chip to two beakers of DI water for 30 seconds each, to gradually remove the developer solution from the chip. Lastly, the chip is rinsed in isopropanol and dried with a N_2 gun for cleaning purposes.

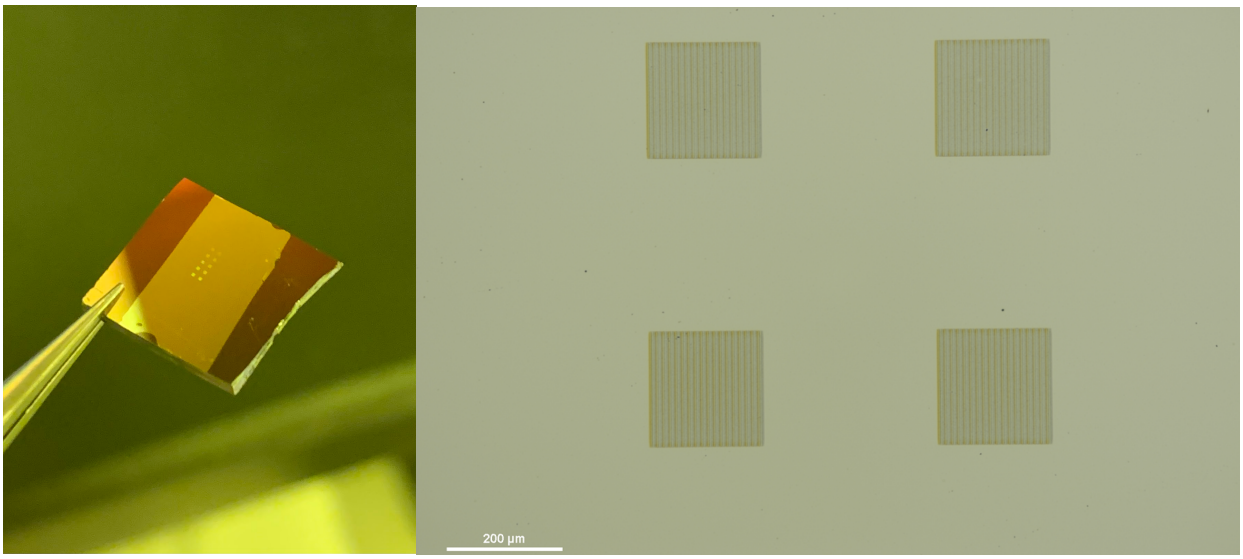

Figure 7: Result of patterning. Left: Visual image of imprinted pattern on the entire material stack. Right: Optical microscope image of pattern. Pattern size of 200 µm across.

Step IV: Pattern Etch

A Cl_2/BCl_3 inductively coupled plasma etch was performed to transfer the pattern into the Al hard mask. This was done using the PT-MTL tool in SNF with the recipe labeled "SNF-Al etch-600nm_min." Blanket films of Al on Si chips were completely removed after 30 seconds of processing with this recipe. This time was chosen to ensure a 150% overetch given the film thickness. The patterned diamond samples were processed using this recipe for 45 seconds to ensure complete removal of the Al film not masked by the HSQ pattern. After this etch, the diamond film underneath the Al film also appeared to have been etched, as evidenced by a color change of the film.

Because of this, we decided not to proceed with the subsequent O_2/Ar etch to transfer the pattern into the diamond, as we suspected that the Cl_2 etch had already etched some diamond. After the Cl_2 etch, the sample was characterized using the Nova SEM in the nanopatterning clean room. The rough surface, low contrast, and no Al mask, confirmed pattern transfer into the diamond.[5] The removal of the Al hard mask from the diamond bars is hypothesized to occur due to corroding by residual Cl_2 in the HSQ after the Cl_2 etch. Before imaging in the SEM, the samples were cleaned in solvent, which removed the remaining corroded Al.

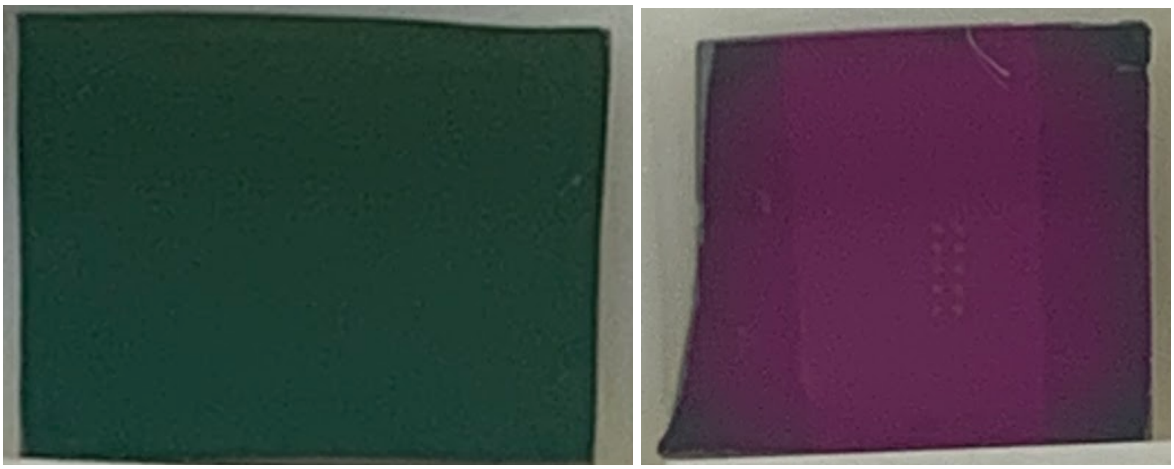

Figure 8: Images of diamond chip both before and after etch. Left: Unetched diamond chip. Right: Patterned diamond chip after 45 second Cl_2 etch

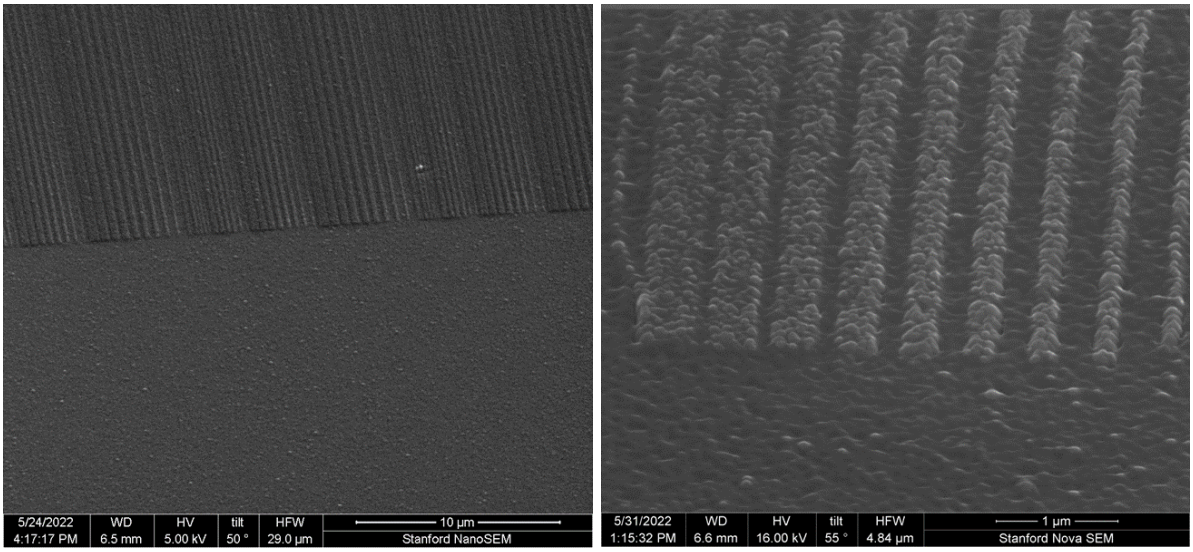

Figure 9: SEM images of diamond metasurface following etch. Left: Zoomed out image of edge of bars. Right: Zoomed in image of individual bars, demonstrating polycrystalline roughness.

The SEM images shown above (in Fig. 9) demonstrate pattern transfer through the Al mask and into the diamond with good resolution. While the images show rough diamond structures, the pattern transfer appears to have occurred with good resolution, as the smallest features, with width of 25 nm, were clearly distinguishable. The roughness of the structures comes from the diamond samples that were used, which were a 100 nm thick film of very rough, polycrystalline diamond. Given the results observed, we believe that higher quality structures can be fabricated using smoother, single crystal samples.

Given that the Cl_2 etch removed the aluminum hard mask during this step, the masking material that preserved the pattern was actually the HSQ. This demonstrated that for

short etches of thin diamond films, HSQ alone might be a good enough hard mask, depending on the length and thickness of the desired etch.[6] Future experiments will entail accurate measurements and calibration of the etch rates of HSQ and diamond to determine the etch selectivity using a chlorine based etch and the maximum thickness of diamond that can be etched with this chemistry based on the selectivity of the etch. We believe that for longer etches, a hard mask and subsequent O_2/Ar etches will be required.[7]

Lessons Learned

The process demonstrated within this report is a result of nearly a quarter of a year of debugging and optimization. Of note, the initial process proposed for this research underwent major modification to its final form utilized today. As can be seen in Figure 10, the original proposal leveraged a silicon dioxide hard mask without any metal mask as well as differing etch steps; subsequent iterations also came and went. Below are some of the critical lessons learned from this process.

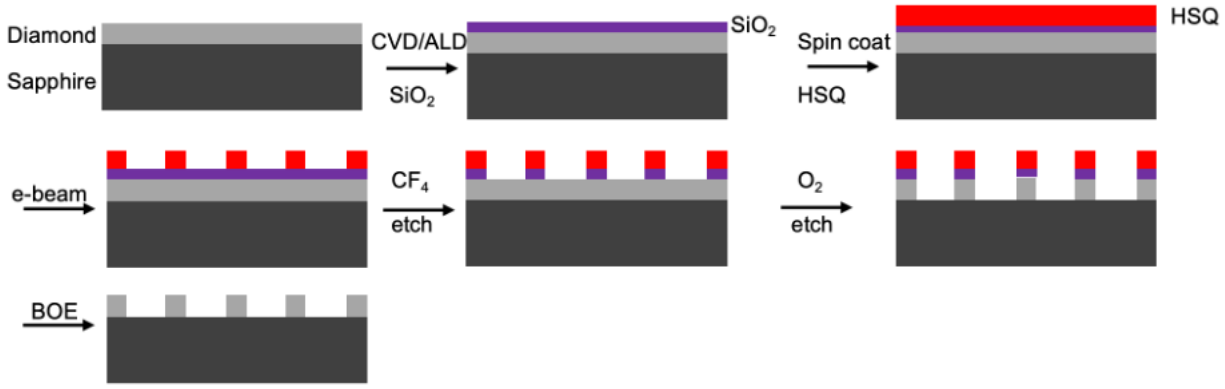

Figure 10: Original process proposed for E241 diamond etch. Major changes were made over the course of the research period.

Lesson Learned #1: Using a Metal Mask and no SiO_2

The initial proposal suggested using SiO_2 as a hard mask upon which the HSQ would be spun. This process was intended to allow for the formation of an adhesion layer for the HSQ to bond to that was not dissimilar in character to the e-beam exposed regions of the HSQ.

However, in an early suggestion from the mentor team, it was proposed that a metal deposition be performed to serve as a hard mask as well. Such a mask, in light of diamond's toughness, would allow for a longer mechanical sputter style etch to be performed without risking removal of the mask. The new material stack, as a result,

would be HSQ on silicon dioxide on Chromium / Aluminum on diamond. While a more complicated process, the thought was that this mask would serve to give the best opportunity at etching away the diamond while maintaining the mask.

Initial results proved promising, with blanket etches of Chromium going as anticipated. However, an issue was encountered when actually patterning samples with silicon dioxide on the chromium. Namely, apparent oxidation of the chromium led to an inability to transfer the pattern into the metal mask; chromium oxide, an even better hard mask than chromium itself, was formed in the process of depositing the silicon dioxide layer.

Consequently, to debug this step, the silicon dioxide was eliminated from the stack completely. This removed the oxidation, allowing the etch to proceed as desired.

Lesson Learned #2: Using a Thicker Metal Mask

Original plans, when swapping to the metal mask, called for 20 nm depositions. However, the patterns created disappeared far too quickly with such thin layers. As a consequence, a much thicker deposition, in this case of Aluminum, was used in the final process. Target thickness of 200 nm were achieved. Note that Aluminum was switched to from Chromium half way through our investigation due to observed use of it as a hard mask in diamond etching specifically in the literature; Chromium may still work, but we proceeded with what had been a demonstrated process.

Lesson Learned #3: Chlorine Etches Diamond

As discussed earlier in the report, the original intent was to proceed with an etch of the metal using chlorine and boron trichloride plasma followed by an oxygen plasma etch of the diamond. However, in etching the metal, it was found that the pattern had already transferred into the diamond as well, meaning that the oxygen etch step could be potentially removed. It is important to note that additional process improvement can be had in ensuring that etch rates are such that the diamond is sufficiently etched before the mask disappears. However, in subsequent review of the literature, reference to chlorine as a diamond etchant was discovered; however, its use is not well documented or leveraged in much of the literature, so this discovery proved valuable in our analysis of the materials stack.

Lesson Learned #4: HSQ is potentially enough of a Chlorine mask

With the discovery that chlorine etched diamond, and at the time of this report, further analysis is being done as to if the metal mask is even needed given HSQ being relatively selective against Chlorine. It is possible that the metal mask at large could be

theoretically removed; however, additional testing needs to be done to validate if this is actually the case.

Future Work and Conclusions

In conclusion, the work done for this project demonstrated that it is possible to pattern diamond films or substrates following a simple procedure that leverages few tools available at the SNF and SNSF facilities. The final process flow follows a fabrication process which resembles the one used for fabrication of silicon photonic devices.

Future work includes calibration of the etch rates of diamond, aluminum, and HSQ during the chlorine etch, and determining whether the aluminum hard mask is necessary for etching thin diamond films. In addition, for longer etches of thicker diamond films, optimization of the O_2/Ar ratio will be required to maintain a high etch selectivity to diamond over the masking material, while obtaining a smooth etch profile.

In the near future, we plan to fabricate beamsteering metasurfaces for visible wavelengths on higher quality, single crystal diamond samples using the process that was developed in this class. Our plans moving forward include performing transmission measurements to characterize the diffraction efficiency, and eventually fabricate high quality factor resonant metasurfaces for applications in quantum sciences and biomarker sensing.

Acknowledgements

Part of this work was performed at the Stanford Nano Shared Facilities (SNSF), supported by the National Science Foundation under award ECCS-2026822.

Work was performed in part in the nano@Stanford labs, which are supported by the National Science Foundation as part of the National Nanotechnology Coordinated Infrastructure under award ECCS-1542152.

Special thanks to the fellow members of E241 as well as our mentors. Particular thanks to Vijay Narsimhan, J Provine, Lavendra Mandyam, Roger Howe, Jihyun Baek, and all the other mentors that provided class feedback. Further thanks to the support from our fellows in the Dionne lab, particularly Professor Jen Dionne, Sahil Dagli, Jefferson Dixon, Elissa Klopfer, and other members of the nanophotonics subgroup. Finally, thanks to the support from the Chowdhury lab in supplying diamond, including Professor Srabanti Chowdhury and Mohamadali Malakoutian. While those materials have not been used yet, they will prove valuable in subsequent iterations of materials implementation.

Budget

Budget for this class was provided by E241 and c-ShARP. Special thanks to the donors that made this possible.

Budget Items	Matti – SNF	Matti - SNSF	Hamish – SNF	Hamish - SNSF
Training	$237.50	$47.50	$95.00	$0.00
Materials	$8.00	$0.00	$0.00	$0.00
Tool Time	$191.67	$0.00	$321.67	$865.00
Total	$1,766.34			
Remaining Budget ***(As of 5/31/22)***	$3,233.66			

References

1. M. Lawrence, D. R. Barton, J. A. Dionne *Nano Letters* (2018)
2. M. Lawrence et al. *Nature Nanotechnology* (2020)
3. T.-Y. Huang et al. *Nature Communications* (2019)
4. J. Hu, M. Lawrence, J. A. Dionne *ACS Photonics* (2020)
5. C. Lee et al. *Diamond and Related Materials* (2008)
6. D. Park et al. *Journal of Vacuum Science & Technology B: Microelectronics and Nanometer Structures* (2006)
7. M.-L. Hicks, A. C. Pakpour-Tabrizi, R. B. Jackman *Scientific Reports* (2019)